Reactive resonances in $N+N_2$ exchange reaction

Dunyou Wang*†, Winifred M. Huo, Christopher E.
Dateo†,David W. Schwenke and James R. Stallcop
NASA Ames Research Center, MS T27B-1, Moffett Field, CA 94035-1000

(Dated: May 29, 2003)

Abstract

Rich reactive resonances are found in a 3D quantum dynamics study of the N + N_2 exchange reaction using a recently developed *ab initio* potential energy surface. This surface is characterized by a feature in the interaction region called 'Lake Eyring', that is, two symmetric transition states with a shallow minimum between them. An L^2 analysis of the quasibound states associated with the shallow minimum confirms that the quasibound states associated with oscillations in all three degrees of freedom in 'Lake Eyring' are responsible for the reactive resonances in the state-to-state reaction probabilities. The quasibound states, mostly the bending motions, give rise to strong reasonance peaks, whereas other motions contribute to the bumps and shoulders in the resonance structure. The initial state reaction probability further proves that the bending motions are the dominating factors of the reaction probability and have longer life times than the stretching motions. This is the first observation of reactive resonances from a 'Lake Eyring' feature in a potential energy surface.

* Electronic mail: dywang@nas.nasa.gov
† Eloret Corporation

Nitrogen is the major constituent of both the Earth's and Titan's atmospheres. Consequently the physics of nitrogen collisions plays an important role in the high speed entry of any space objects into these atmospheres. The temperature of the shock wave introduced by the high-speed entry can be as high as 20,000K. The radicals, atoms and ions so produced are chemically reactive and subsequent reactions can proceed rapidly. Both the exchange and dissociation reactions of $N + N_2$ are among the list of chemical reactions needed for flow field modeling and heat shield design for future space missions such as sample return from a Mars mission and aerocapture of a space capsule in Titan's atmosphere. Experimental measurements of chemical reaction rates at such high temperatures are difficult to carry out and extrapolations from lower temperature data are unreliable. While state-to-state cross sections can be measured using molecular beam experiments, so far no such experiments have been reported for $N + N_2$ reactions due to the lack of an adequate N atom beam source. Thus theoretical calculations provide the only available means to determine the required data. The time-dependent quantum dynamics study of the $N + N_2$ exchange reaction reported in this letter contributes to the necessary database for flow field characterization.

Reactive resonances [1, 2] have been studied intensively since they were found in theoretical studies of gas phase reactions[3–5]. Very recently these reactive resonances have been observed in experimental studies of these reactions, $H + D_2 \rightarrow HD + D$ [6], $H + HD \rightarrow D + H_2$ [7] and $F + HD \rightarrow HF + D$ [8]. There are three previously known types of reactive resonances established from scattering calculations. The first type is the transition state resonances, a result of dynamically trapped vibrational levels of the transition state, such as the reactive resonances in the reactions of $H+H_2$, $F+H_2$ and their deuterated variants[6–8]. The second is the result of quasibound states localized in the van der Waals well of either the entrance or exit channel, such as the resonances in O + HCl reaction[9]. The third type occurs when the reacting system has a chemically bound state with a barrier to the asymptote. The quasibound states trapped in the potential well region give rise to resonances. An example is the $O + O_2$ exchange reaction[10]. The present study investigates a new type of reactive resonance where quasibound states are trapped in 'Lake Eyring' feature in the interaction region high above the asymptote, with all three vibrational motions contributing to the resonances, not only two vibrational motions.

The first quantum dynamics study of the cumulative reaction probabilities and chemical reaction rates of the $N+N_2$ exchange reaction, as well as the first *ab initio* potential energy

surface(PES) for the N_3 system, have been reported by this group[11]. This PES, determined using high level quantum chemistry calculations, is characterized by two nonlinear transition states in the interaction region that are equivalent to each other by the interchange of two N atoms, as well as a shallow well between the two transition states. Their geometries are $r_a(r_b) = 2.23$ bohr, $r_b(r_a) = 2.80$ bohr and $\Theta = 119^o$ for the transition states, and $r_a = r_b = 2.40$ bohr and $\Theta = 120^o$ for the minimum, with r_a and r_b the two N-N bonds and Θ the bond angle. The transition state is located at 2.05 eV above the energy of of N + N_2 at the asymptote, and the shallow minimum is at 1.90 eV. The double hump shape of N_3 PES in the interaction region with two transition states and a shallow minimum (See Fig.1 in Ref.[13]) has been previously termed 'Lake Eyring' [12, 13]. Up to now no dynamics studies have ever been performed to investigate the reactive resonances from this type of structure in the PES. In this letter, we report the first state-to-state quantum calculations of the exchange reaction N+N_2 and study the reactive resonances due to this unique feature of the PES.

A quantum time-dependent wavepacket method [14, 15] is employed here to study the state resolved properties of N+N_2. The split-operator propagation scheme is used for wave packet propagation and a two stage propagation approach is employed in this study. First, an initial wave packet(for a given total angular momentum J) which is located in the reactant asymptotic region, covering the translational energy from 2.0 eV to 3.2 eV, is propagated in the reactant Jacobi coordinates on the *ab initio* N+N_2 PES. After about 2,000 atomic units of time the wave packet reaches the interaction region ('Lake Eyring' region). The wave packet is transformed from the reactant Jacobi coordinates into the product Jacobi coordinates, and then propagated in the product channel on the PES . After the wave packet enters the asymptotic region, the energy-dependent state-resolved reaction probability $P^J_{fi}(E)$ is extracted by evaluating the flux through a dividing surface in the product asymptotic region,

$$P^J_{fi}(E) = |S_{fi}|^2 = \frac{\hbar}{\mu_p} Im[\Psi^{+*}_{fi}(E,R)\frac{\partial}{\partial R}\Psi^{+}_{fi}(E,R)]|_{R=R_f}, \qquad (1)$$

where μ_p is the reduced mass of the system in the product channel and R the translation Jacobi coordinate that connects one N atom to the center mass of the N_2 molecule. Also R_f is the position of the dividing surface in the product asymptotic region where the final state interaction is over and the flux is invariant to the change in R_f. $\Psi^{+}_{fi}(E,R)$ is the scattering wavefunction.

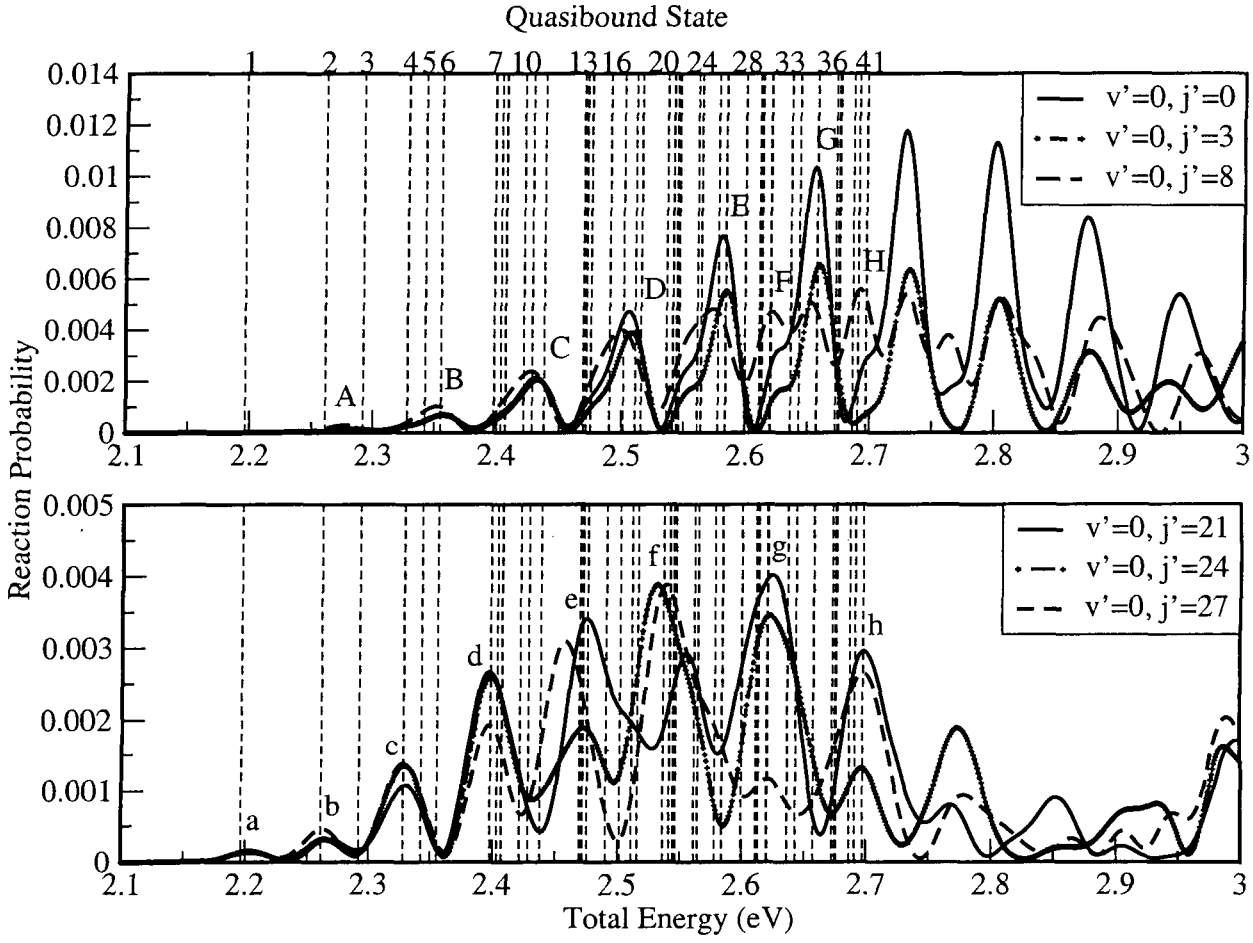

FIG. 1: State-to-state reaction probabilities for exchange reaction N+$N_2(\nu = 0, j = 0) \rightarrow N_2(\nu', j')$+N as a function of total energy for total angular momentum $J = 0$. The eigenvalues of the quasibound states from the 'Lake Eyring' structure are indicated as vertical lines.

Since a two stage propagation scheme is employed in the calculation, two sets of basis functions are used. One set is in the reactant channel, 220 sine functions to expand the translational coordinate R from 2.3 a_0 to 10.4 a_0, 100 vibrational eigenfunction of N_2 to cover the vibrational coordinate r from 1.3 a_0 to 5.5 a_0, and 70 even Legendre functions(j_{max}=140) or 70 odd Legendre functions (j_{max}=139) for the angular part θ. The second set is for the product channel. Here 320 sine functions are used for the translation coordinate R' ranging from 0.1 a_0 to 14.0 a_0, 220 vibrational functions to expand the vibrational coordinate r', from 0.1 a_0 to 12.0 a_0, and 150 Legendre functions for θ'. The state resolved flux is calculated at R_f=10.0 a.u. The scattering calculation has been carried out using 32 CPU on an Origin 3000 system, In total, about 40,000 CPU hours were used for the state resolved calculations.

Figure 1 shows the state-to-state reaction probabilities from the initial $\nu = 0, j = 0$ state to different final states with total angular momentum $J = 0$. Dramatic reactive resonances are seen in these state-to-state reaction probabilities. In order to establish the origin of these resonances, we search for the metastable states associated with the shallow minimum in 'Lake Eyring' for $J = 0$. The calculations are done by diagonalizing the 3D complex Hamiltonian matrix using the L^2 method with an absorbing potential in the reactant channel[9]. The stationary eigenvalues are identified as be the quasibound states, and the real and imaginary parts of these eigenvalues give the resonance energies and widths. The 'Lake Eyring' feature is located in both reactant and product channels, but the absorbing potential is confined in the reactant channel; hence, the resonance widths given by the present quasibound calculation are not meaningful and not listed. Table I lists the lowest set of metastable states found in the minimum up to vibrational mode (0,7,0). The metastable states at higher energies cannot be assigned due to the strong coupling between the bending and stretching motions. Note that all the metastable states are quasibound states since they lie above the transition state energy 2.05 eV. Their eigenvalues are plotted as vertical lines in Fig.1, to be compared with the resonance structures in the state-to-state reaction probabilities.

In the upper part of Fig.1, most resonance peaks coincide with the eigenvalue of a particular quasibound state. For example, peak group B at 2.36 eV corresponds to the eigenvalue of the (0,1,1) quasibound state. Similarly peak group C is located at the eigenvalue of (1,0,1), E at (1,2,1), F at (0,6,0), G at (1,3,1) and H at (1,5,0) quasibound states. Note most of the resonances are not symmetric. For example, the left side of peak group C, has a small shoulder, and is broader than the right side. This is due to the fact that contributions to the left side of this resonance structure come from 4 quasibound states, (0,3,0), (0,0,2), (1,1,0) and (0,2,1), whereas only one quasibound state (0,1,2) is located at the right of the peak structure. Also, three closely spaced quasibound states (0,3,0), (0,0,2) and (1,1,0) are located exactly at the shoulder position. In a similar manner, the features observed in peak groups B, D, E, F and G are also attributable to the quasibound states in Table I. Peaks A and H are more symmetrical due to one quasibound state each located at two sides. The present analysis shows that all resonance structures in the figure come from the quasibound states in the 'Lake Eyring' feature, with some quasibound modes giving rise to strong resonance peaks whereas others contribute to the 'bumps' and 'shoulders' of these

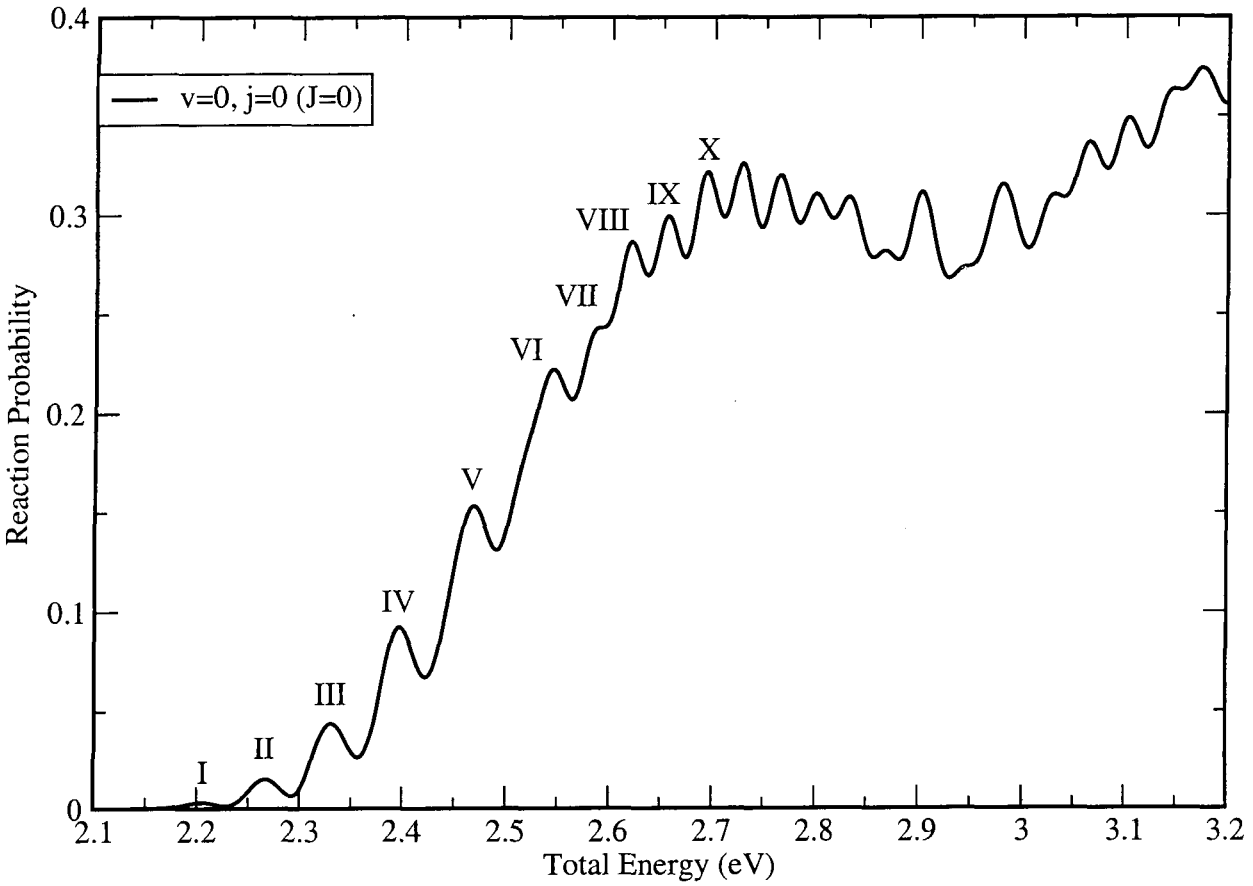

FIG. 2: Initial state selected reaction probability for $N+N_2(\nu = 0, j = 0)$ as a function of total energy for J=0.

resonances.

Similar features are found in the lower part of Fig.1. The eigenvalues of the dominant quasibound states are located right at the resonance peaks, such as (0,0,0) at the *a* peak group, (0,1,0) at the *b* peak group, (0,2,0) at the *c* peak group. Also the eigenvalues of (0,3,0), (1,2,0), (0,2,2), (1,4,0) and (0,7,0) are located at the center of other peaks. Note that most peaks are donimated by the pure bending modes or the combination of bending and stretching modes. Other quasibound states not associated with the bending mode contribute to the 'bumps' and 'shoulders' in the resonance structure, but generally not strong peaks. Through the assignments of all final state resonances, it is found that the bending motion and bending motion coupled with stretching motion are the dominating factors of the reactive resonances. Detailed assignments will be published in a future paper.

TABLE I: Quasibound states associated with the minimum in the 'Lake Eyring' feature in the N_3 potential energy surface and resonance peaks in the initial state selected reaction probability (fourth and fifth columns).The zero of the tabulated energy is the N+N_2 asymptote.

Res. No.	$(\nu_R, \nu_\theta, \nu_r)$	quasibound(eV)	peak	peak pos.(eV)
1	(0,0,0)	2.196	I	2.205
2	(0,1,0)	2.261	II	2.267
3	(0,0,1)	2.292		
4	(0,2,0)	2.328	III	2.330
5	(1,0,0)	2.343		
6	(0,1,1)	2.355		
7	(0,3,0)	2.398	IV	2.396
8	(0,0,2)	2.404		
9	(1,1,0)	2.407		
10	(0,2,1)	2.422		
11	(1,0,1)	2.428		
12	(0,1,2)	2.438		
13	(0,4,0)	2.469	V	2.468
14	(1,2,0)	2.472		
15	(0,0,3)	2.476		
16	(0,3,1)	2.491		
17	(2,0,0)	2.502		
18	(1,1,1)	2.511		
19	(0,2,2)	2.516		
20	(1,0,2)	2.536		
21	(1,3,0)	2.541		
22	(0,5,0)	2.545	VI	2.544

Res. No.	$(\nu_R, \nu_\theta, \nu_r)$	quasibound(eV)	peak	peak pos.(eV)
23	(2,1,0)	2.546		
24	(0,4,1)	2.561		
25	(0,3,2)	2.564		
26	(1,1,2)	2.578		
27	(1,2,1)	2.584	VII	2.591
28	(2,0,1)	2.599		
29	(0,1,3)	2.611		
30	(1,4,0)	2.613		
31	(0,2,3)	2.620		
32	(0,6,0)	2.620	VIII	2.620
33	(0,5,1)	2.636		
34	(2,2,0)	2.643		
35	(1,3,1)	2.657	IX	2.656
36	(3,0,0)	2.673		
37	(1,0,3)	2.675		
38	(1,1,3)	2.676		
39	(0,4,2)	2.686		
40	(1,5,0)	2.691		
41	(0,7,0)	2.697	X	2.693

Figure 2 presents the initial state reaction probability for $v = 0$, $j = 0$ at $J = 0$. The initial state reaction probability is obtained by summing over all the final states for a given initial state. Features of reactive resonances are also observed in this spectrum but the summation has washed out the sharp features in the state to state reaction probabilities. Besides the (0,0,0) state, only quasibound states with excited bending modes or combined bending and stretching modes have correspondence in the resonance peaks below 2.7 eV. (See the fourth and fifth columns of Table I). All other features, observable in the state to state reaction probability in Fig. 1, are washed out because they are much weaker. The dominance of bending resonance is not surprising. The bond angles of the minimum and

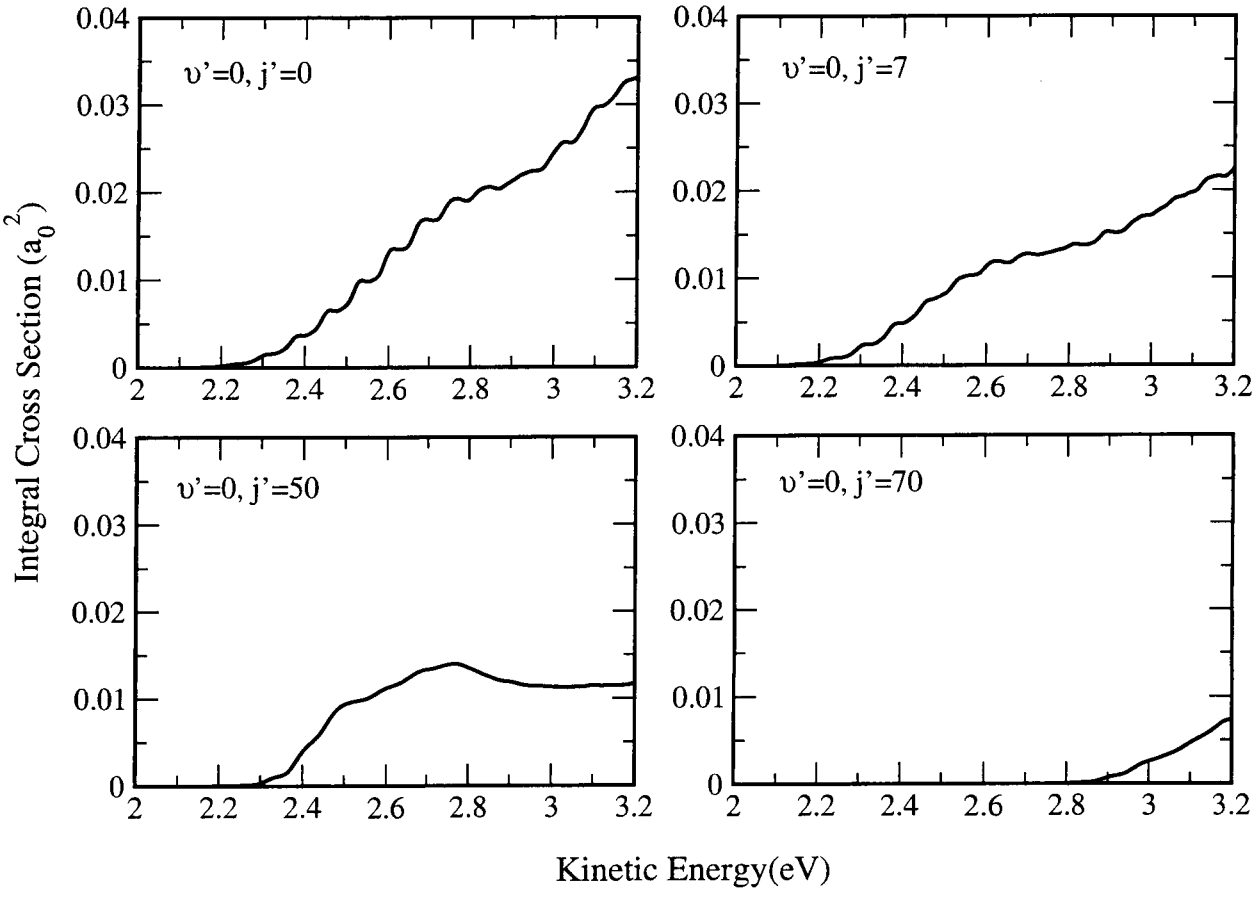

FIG. 3: State to state integral cross sections for exchange reaction of $N+N_2$ for the ground initial ro-vibrational state to different final ro-vibrational states, $N+N_2(\nu = 0, j = 0) \rightarrow N_2(\nu', j')+N$, as a function of the kinetic energy.

transition states are very close, but the bond distances are different. Stretching motions take the wave functions out of 'Lake Eyring' into final products, whereas bending motions are more likely to keep the wave functions in the 'Lake Eyring' region, resulting in a longer lifetime. Since the resonances in Figs. 1 and 2 are caused by the 'Lake Eyring' feature in the potential energy surface, we name them Eyring resonances.

The state to state integral cross sections are given by

$$\sigma_{v'j' \leftarrow vj} = \frac{\pi}{k^2(2j+1)} \sum_{J=0} (2J+1) P^J_{v'j' \leftarrow vj}(E). \tag{2}$$

This calculation is done by summing over 95 (J_{max}=95) partial waves for the kinetic energy range from 2.0 eV to 3.2 eV. Fig.3 shows the converged state to state integral cross sections from the initial ro-vibrational state ($\nu = 0$, $j = 0$) to different final ro-vibrational

states. The dramatic resonances in the state-to-state reaction probabilities for a given total J barely survive the sum over partial waves. Nonetheless,the resonances for the lower final ro-vibrational states, such as ($\nu' = 0$, $j' = 0$) and ($\nu' = 0$, $j' = 7$) states, show up as 'bumps'. They are much broader than in the spectrum of Fig.1, but still observable. However, for higher final ro-vibrational states, for example for the ($\nu' = 0$, $j' = 50$) and ($\nu' = 0$, $j' = 70$) the resonances have been washed out by the sum of the partial waves. Fig.3 also shows that the integral cross section for $j = 0 \rightarrow j' = 7$ is approximately the same magnitude as that for $j = 0 \rightarrow j' = 50$, but the cross section for $j = 0 \rightarrow j' = 70$ is much smaller. In view of the magnitude of the cross sections to high j' such as $j = 0 \rightarrow j' = 50$, it appears that the N + N_2 exchange reaction is quite efficient in providing significantly high rotational levels, a result relevant to the question of energy partitioning in entry physics.

In conclusion, the time-dependent full 3D accurate quantal approach is carried out to study the reactive resonances in the state resolved exchange reaction of N + N_2. Dramatic resonances are found in the state-to-state reaction probabilities; these resonances originate from 'Lake Eyring' quasibound states, with the bending motions dominating the resonance peaks, and other vibrational motions contributing to the shoulder and bumps in the resonance structure. Eyring resonances are also observable in the initial state selected reaction probability, but mainly the bending modes survive the summation of all final ro-vibrational states, confirming the conclusion that resonances from the bending modes dominate Eyring resonances in this reaction. While the summation over partial waves in the state-to-state integral cross section washes out the sharp resonances, the bumps in the integral cross section for low j' excitations are observable and may be used to establish the resonances in future experiments. The resonance enhancement in the exchange cross section also produces high final j' levels. Thus they should be taken into account in the flow field modeling.

This work was partially supported by NASA's Office of Space Science, 344-38-12-16. D.Y.W. and C.E.D. acknowledge support from NASA prime Contract No. NAS2-0062.

---

[1] G. C. Schatz Science **288**, 1599 (2000).

[2] F. Fernandez-Alonso and R. N. Zare, Annu. Rev. Phys. Chem. **53**, 67 (2002).

[3] R. D. Levine and S. -F. Wu, Chem. Phys. Lett. **11**, 557 (1971).

[4] D. G. Truhlar and A. Kuppermann, J. Chem. Phys. **56**, 2232 (1972).

[5] G. C. Schatz and A. Kuppermann, J. Chem. Phys. **59**, 964 (1973).

[6] B. K. Kendrick, L. Jayasinghe, S. Moser, M. Auzinsh and N. Shafer-Ray, Phys. Rev. Lett. **84**, 4325 (2000).

[7] R. T. Skodje, D. Skouteris, D. E. Manolopoulous, S. Lee, F. Dong and K. Liu, J. Chem. Phys. **112**, 4536 (2000).

[8] S. D. Chao, S. A. Harich, D. X. Dai, C. C. Wang, X. Yang and R. T. Skodje, J. Chem. Phys. **117**, 8341 (2002).

[9] T. Xie, D. Y. Wang and J. M. Bowman, J. Chem. Phys. **116**, 7461 (2002).

[10] P. Fleurat-Lessard, S. Yu. Grebenshchikov, R. Siebert, R. Schinke and N. Halberstadt, J. Chem. Phys. **118**, 610 (2003).

[11] D. Y. Wang, J. R. Stallcop, W. M. Huo, C. E. Dateo, D. W. Schwenke and H. Partridge, J. Chem. Phys. **118**, 2186 (2003).

[12] H. Eyring, J. Walter, and G. E. Kimball, *Quantum Chemistry*, J. Wiley and Sons, New York (1944).

[13] M. Mladenović, P. Botschwina, P. Sebald, and S. Carter, Theor. Chem. Acc. **100**,, 134 (1998).

[14] D. H. Zhang and J. Z. H. Zhang, J. Chem. Phys. **101**, 3671 (1994).

[15] W. Zhu, D. Y. Wang and J. Z. H. Zhang, Theor. Chem. Acc. **96**, 31 (1997).

[16] S. Sukiasyan and H. -D. Meyer J. Phys. Chem. A **105**, 2604 (2001).